

---

# Morphology and Kinematics of the Bipolar Post-AGB Star IRAS 16594-4656

G. C. Van de Steene<sup>1</sup>, T. Ueta<sup>2</sup>, P. A. M. van Hoof<sup>1</sup>, M. Reyniers<sup>3</sup>, and A. G. Ginsburg<sup>4</sup>

<sup>1</sup> Royal Observatory of Belgium, Ringlaan 3, 1180 Brussels, Belgium  
gsteene@oma.be, pvh@oma.be

<sup>2</sup> Department of Physics and Astronomy, University of Denver, Denver, CO 80208, U.S.A. tueta@du.edu

<sup>3</sup> Instituut voor Sterrenkunde, K.U. Leuven, Celestijnenlaan 200D, 3001 Leuven, Belgium maarten.reyniers@ster.kuleuven.be

<sup>4</sup> Department of Astrophysical and Planetary Sciences, University of Colorado, Boulder, CO 8039, USA

**Summary.** IRAS 16594-4656 is a C-rich B[e]-type post-AGB star with a strong stellar wind, and maybe a disk. Shocked H<sub>2</sub> reveals the interaction of the post-AGB wind with the AGB shell and the shaping of the hollow bipolar shell. The shocked [Fe II] 1.645 μm emission line originates in the stellar wind, or possibly in a disk, close to the central star. The [O I] and [C I] emission lines in the optical spectrum indicate the presence of a very high density region.

**Key words:** infrared: stars: post-AGB, individual: IRAS 16594-4656

## 1 Introduction

IRAS 16594-4656 is a post-AGB star of spectral type B7 ( $T_{\text{eff}} = 14,000$  K) [10, 6], which has not evolved to the PN stage yet [9]. It is C-rich and shows the 21 μm feature in its ISO spectrum [2]. The HST WFPC2 image in the optical shows a bipolar reflection nebula, which has 3 extensions on each side [3]. The outer nebula shows concentric arcs [4]. High resolution mid-infrared images in the N and Q band show an equatorially enhanced distribution of dust, which is geometrically thinner at the center than at the edges, and a pair of bipolar lobes, which show a close correspondence with the HST H<sub>2</sub> map [12]. Polarization data show that the inner structure is hollow, bipolar, and elongated ( $5'' \times 2''$  at PA 80°) [8]. [11] showed the presence of shock excited [Fe II] 1.645 μm and H<sub>2</sub> emission.

## 2 Observations

High resolution near infrared spectra of  $\text{H}_2$  1-0S(1),  $[\text{Fe II}]$  1.645  $\mu\text{m}$ , and  $\text{Pa}\beta$  were obtained with the Phoenix instrument on Gemini South in 2003. Optical echelle spectroscopy was performed with UVES on the VLT in 2000 [6]. Slit positions are shown in Fig. 1.

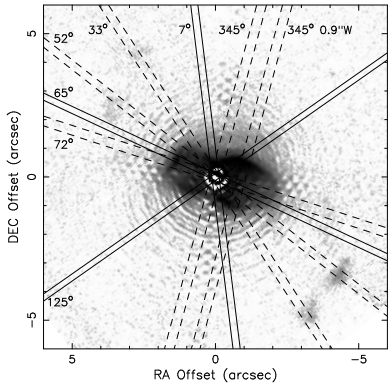


**Fig. 1.** The HST/NICMOS  $\text{H}_2$  1-0S(1) image showing the slit positions through the central star of our data at  $7^\circ$ ,  $65^\circ$  and  $125^\circ$  with  $0''.25$  slit width (solid lines) and data from [5] at  $33^\circ$ ,  $52^\circ$ ,  $72^\circ$ ,  $345^\circ$ , and  $345^\circ$  offset  $0''.9$  W with  $0''.34$  slit width (dashed lines). The UVES slit was orientated E-W and had a width of  $0''.70$ .

## 3 Results

### 3.1 Near Infrared Spectroscopy

Fig. 2 shows the  $[\text{Fe II}]$  contours overplotted on the  $\text{H}_2$  position-velocity diagram. The  $[\text{Fe II}]$  and  $\text{H}_2$  emission clearly originate in different regions. The shocked  $\text{H}_2$  emission traces the interaction between the post-AGB wind and the AGB shell. The  $[\text{Fe II}]$  emission comes from closer to the central star at all position angles and shows a larger velocity dispersion than the  $\text{H}_2$  emission. The  $[\text{Fe II}]$  emission is extended with a size of 0.004 pc (80 AU) at an assumed distance of 2.2 kpc [11]. The  $[\text{Fe II}]$  emission probably originates in the stellar wind or disk close to the central star.

In order to investigate the 3 dimensional structure, we constructed a velocity cube with all available  $\text{H}_2$  1-0S(1) Phoenix data (our data and data presented in [5]). In Fig. 3 each channel has a width of 5.05 km/s. Maps in our velocity cube near the reference velocity of -29 km/s indicate that the  $\text{H}_2$  emission is strong in both lobes, but stronger in the western lobe than in the eastern lobe. They also indicate that there is in fact less emission in the equatorial region of the shell.

Fig. 4 shows the 3D surface constructed based on the  $\text{H}_2$  data cube at 30% of the peak emission assuming a homologous expansion (i.e. velocity

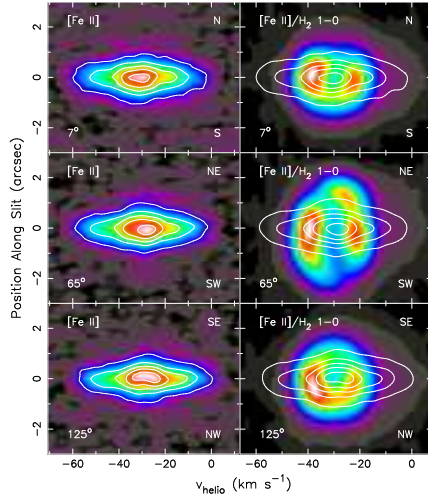


**Fig. 2.** The  $[\text{Fe II}]$   $1.645 \mu\text{m}$  contours are overlotted on the  $[\text{Fe II}]$  position-velocity image (left) and on the  $\text{H}_2$  1-0S(1) position-velocity image (right). The vertical axis shows the position along the slit and the horizontal axis the heliocentric velocity.

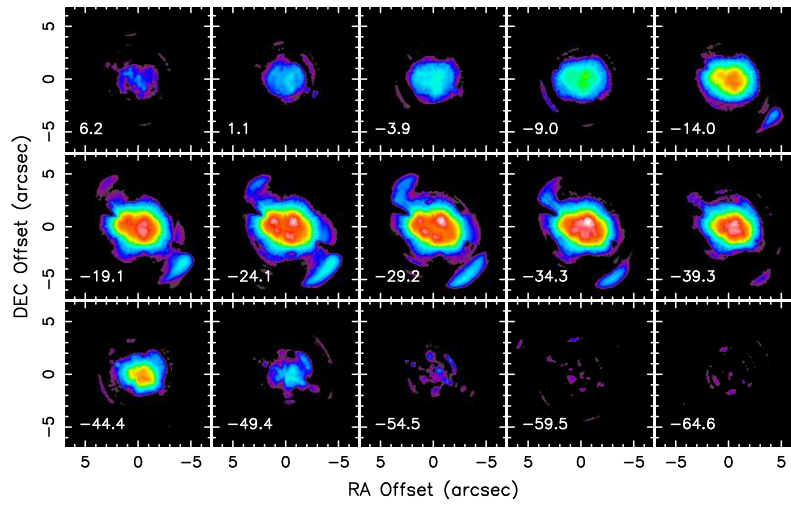


**Fig. 3.** The data cube constructed using all existing spectra of  $\text{H}_2$  1-0S(1). Each channel has a width of  $5.05 \text{ km/s}$ . The central velocity in each channel is indicated at the bottom left corner of each subimage in  $\text{km/s}$ .

proportional to the distance to the star). The overall 3D structure in  $\text{H}_2$  is such that the  $\text{H}_2$  emission is distributed in a bipolar shell. The 3D volume shows the central cavity that is responsible for the hollow appearance of the shell along the polar axis of the bipolar lobes, the western and the eastern elongations at the approaching and the receding sides of the shell, and the holes on the surface at the top and bottom of the equatorial regions.

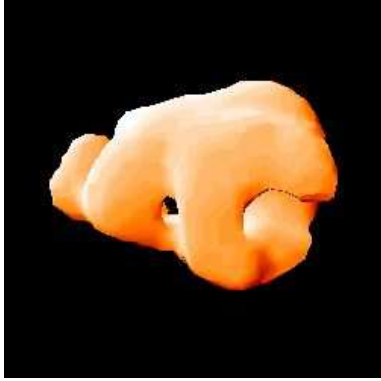


**Fig. 4.** The figure shows the bottom right view of the 3D H<sub>2</sub> surface, illuminated obliquely by a fiducial light source.

### 3.2 Optical Spectroscopy

Because the echelle spectra were obtained with the image slicer, we lack spatial information, but based on their very similar profiles, the optical [O I] and [C I] emission lines seem to originate in the region where the H<sub>2</sub> emission is produced (Fig. 5). No [O II] is detected. Assuming  $6000 \leq T_e \leq 10,000$  K, the dereddened [O I] (6300+6363)/5577 ratio indicates the presence of a high density region of about  $10^7$  cm<sup>-3</sup>.

The H $\alpha$  emission shows a P-Cygni type profile indicating a wind velocity of  $80 \pm 10$  km/s and wings up to 1200 km/s (Fig. 6). The very broad H $\alpha$  wings may be produced by Raman scattering [1]. Other optical absorption lines are mostly asymmetric and show the effect of a stellar wind. Some optical lines such as He I 587.6 nm show a “central quasi emission feature”, which might indicate the presence of a disk [7].

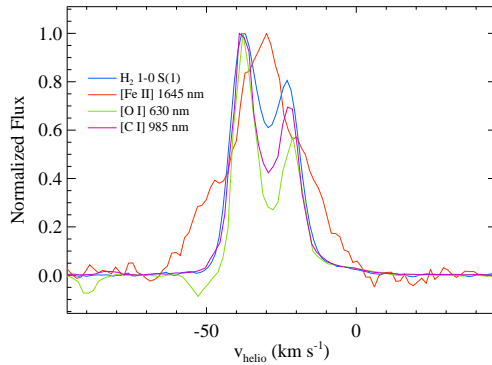


**Fig. 5.** The line profile of H<sub>2</sub> is compared to the line profiles of [O I], [C I], and [Fe II] as indicated. The profiles of [O I], [C I], and H<sub>2</sub> are very similar. The [Fe II] line profile is different.

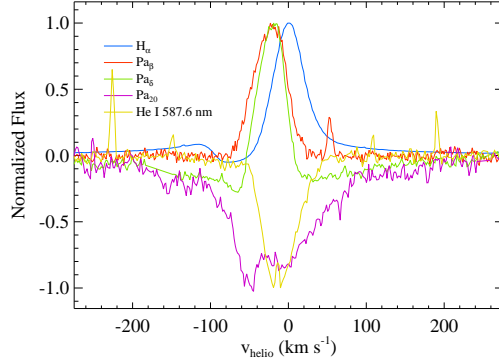


**Fig. 6.** The Balmer, Paschen, and He I 587.6 nm normalized line profiles are plotted to show their asymmetric line shapes and affected by a strong stellar wind.

## 4 Summary

IRAS 16594-4656 is a C-rich B[e]-type post-AGB star with a strong stellar wind, and maybe a disk. Shocked  $\text{H}_2$  reveals the interaction of the post-AGB wind with the AGB shell and the shaping of the hollow bipolar shell. The shocked  $[\text{Fe II}]$  1.645  $\mu\text{m}$  line originates in the stellar wind, or possibly in a disk, close to the central star. The  $[\text{O I}]$  and  $[\text{C I}]$  emission lines in the optical spectrum indicate the presence of a very high density region.

## References

1. Arrieta, Torres-Peimbert: *ApJS*, **147**, 97 (2003)
2. García-Lario, P., Manchado, A., Ulla, A. L., & Manteiga, M.: *ApJ*, **513**, 941 (1999)
3. Hrivnak, B. J., Kwok, S., & Su, K. Y. L.: *ApJ*, **524**, 849 (1999)
4. Hrivnak, B. J., Kwok, S., & Su, K. Y. L.: *AJ*, **121**, 2775 (2001)
5. Hrivnak, B. J., Smith, N., Su, K. Y. L., Kelly, D. M., Kwok, S., & Sahai, R.: in *IAU Symp. 234, "Planetary Nebulae in our Galaxy and Beyond"*, eds. M. J. Barlow & R. H. Méndez (2006), pp 423
6. Reyniers, M.: High resolution spectroscopy of post-AGB stars: AGB nucleosynthesis and dredge-up, PhD Thesis, K.U.Leuven, Belgium, (2002)
7. Rivinius, T., Stefl, S., Baade, D.: *A&A*, **348**, 831
8. Ueta, T., Murakawa, K., & Meixner, M.: *AJ*, **133**, 1345 (2007)
9. Van de Steene, G. C., & Pottasch, S. R.: *A&A*, **274**, 895 (1993)
10. Van de Steene, G. C., Wood, P. R., & van Hoof, P. A. M.: In *ASP Conf. Ser. 199, "Asymmetrical Planetary Nebulae II: From Origins to Microstructures"*, eds. J. H. Kastner, N. Soker, & S. Rappaport (2000), p. 191
11. Van de Steene, G. C., & van Hoof, P. A. M.: *A&A*, **406**, 773 (2003)
12. Volk, K., Hrivnak, B. J., Su, K. Y. L., & Kwok, S.: *ApJ*, **651**, 294 (2006)